JOURNAL OF GEOPHYSICAL RESEARCH, VOL. 104, NO. C12, PAGES 29,721-29,731, DECEMBER 15, 1999

Informational equivalence between synthetic aperture radar imagery and the thickness of Arctic pack ice

Bryan Kerman

Atmospheric Environment Service, Canada Centre for Inland Waters, Burlington, Ontario.

Peter Wadhams and Norman Davis

Scott Polar Research Institute, University of Cambridge, England.

Joey Comiso

Oceans and Ice Branch, NASA Goddard Space Flight Center, Greenbelt, Maryland.

Abstract. The negative exponential form of the conditional probability of both differences in synthetic aperture radar (SAR) intensity and differences in thickness between neighbors is used as the basis of a representation of structural information in terms of textural information for sea ice. The analysis is based on a unique data set involving airborne SAR flights over the track of a submarine that simultaneously profiled ice thickness by means of an upwardly directed sonar. It is shown that both sets of data, namely, imagery and thickness, possess an identical conditional probability relationship. This probability is composed of both a fractal property for spatial separations and a simple negative exponential distribution for intensity or thickness differences for fixed separations. These properties allow for the derivation of two forms of information: textural and structural. An intercomparison of the structural information in terms of the textural information is offered for the same ice field as imaged by a SAR and measured from a submarine for its thickness. It is shown that the information curves for both the imagery and thickness have a similar geometrical form. It is demonstrated that three subranges within the information curves correspond to three visibly identifiable ice types and three thickness ranges associated previously with these ice types. It is suggested that an understanding of the transformation between the two sets of information states might provide estimated statistics of Arctic ice thickness from SAR imagery.

1. Introduction

One of the objectives of existing satellite systems such as ERS 2 and Radarsat is to provide imagery of ice-covered areas to allow ships to plan a passage. The imagery is often downloaded directly to the ship, where it is interpreted by a skilled observer and a path is determined empirically [*Ramsay et al.*, 1998]. To be able to compute such paths automatically, it is desirable that the ice thickness, or at least geophysically relevant information about the nature of the ice cover, be derived from the satellite imagery.

Previous research [*Wadhams and Comiso*, 1992] has shown that a point-to-point correlation of synthetic aperture radar (SAR) image intensity and ice thickness is not meaningful. It is recognized that an estimate of ice thickness will require understanding the extended spatial properties of an ice field. One method of developing estimates of the average thickness of identifiable floes is by automatically recognizing ice type [*Kwok et al.*, 1992] based on its texture [*Holmes et al.*, 1984; *Barber and LeDrew*, 1991; *Shokr*, 1991]. Two common texture parameters used for ice type recognition are the locally averaged variance, as a measure of "energy", and the entropy, as a measure of disorder. (The method discussed below includes both these concepts.). Empirical studies [*Wadhams and Horne*, 1980; *McLaren*, 1989] have developed the relationship between average thickness and ice type.

An inherent weakness of textural models is their inability to recognize structural aspects of the imagery. To some extent, this is ameliorated by the fact that structural information may be correlated with the textural aspects of ice types. For example, there is additional information in the structure or form of certain ice types, such as rounded multiyear floes, elongated

Paper number 1999JC900187.
0148-0227/99/1999JC900187$09.00

leads, and fibrous networks of ridges. Accordingly the texture-only technique displays less skill in segmentation than the results obtained by human ice analysts. It is therefore one of the objectives of this and previously reported results by the author and colleagues to build a structural dimension into ice type recognition.

Spatial properties that are visible in SAR imagery have an interesting and important property for applications; they possess statistics that vary with the separation between pairs of pixels [*Falco et al.*, 1996]. This so-called scaling or fractal property [*Feder*, 1988] within imagery was shown in an early ice recognition system [*Pentland*, 1984] to be more powerful than a combination of textural parameters in identifying ice type such as leads and ridges. It is also known that the fractal property is related to the strength of the ice itself on different scales [*Duxbury and Li*, 1990; *Palmer and Sanderson*, 1991]. The correspondence between fractal properties in imagery and in physical properties of ice, such as its strength and thickness, has not been hitherto exploited.

Recently, the statistics of intensity differences between neighbors [*Kerman*, 1998a; *Kerman and Johnson*, 1998] for some SAR imagery of sea ice in the Beaufort Sea [*Drinkwater et al.*, 1991] have been reported. Kerman and Johnson [1998] show that the probability of a difference in intensity between neighbors (a fixed distance apart) follows a (negative) exponential distribution. This property is called the "Gibbs" property because it is possible [*Kerman*, 1998a] to make an analogy between the energetics of a classical, statistically defined system of distributed energy and variability in intensity in the imagery. Further, it was also shown that the probability of finding a fixed intensity difference between pixels at a given separation is a simple algebraic ("power law") function of the separation. This hyperbolic relationship with spatial separation is variously referred to hereafter as "fractal" or "scaling".

These two results, fractal and Gibbsian, can be written in a combined form as

$$p_c(\Delta I; I) = [Q_1(I)\lambda^{m(I)}]^{-1} exp[-\beta(I)\Delta I] \qquad (1)$$

for the conditional probability p_c of a given intensity difference ΔI between pixels, the most intense being separated from a pixel at intensity I by a given spatial separation λ. It is emphasized that parameters Q_1, m, and β are empirical functions of I derived from the analysis.

In another recent paper. Kerman [1999] shows that if (1) is subjected to a logarithmic transformation and ensemble averaging, i.e.,

$$- < lnp_c(\Delta I; I) > = lnQ + \beta < \Delta I > \qquad (2)$$

(where $Q = Q_1\lambda^m$), the result can be identified as a statement of the decomposition of the entropy $- < lnp_c >$ within the image. Of the terms constituting the decomposition, the expression lnQ is shown there to characterize "structural" entropy and the expression $\beta < \Delta I >$ is shown to represent the "textural" entropy. Shannon's [1948] famous result allows us to equate information and entropy.

To grasp how this decomposition arises, it is useful to consider a simple experiment. A black ($I = 0$) mask is placed over an image of sea ice. As a single pixel is displayed, the "surprise" associated with a nonblack pixel will be proportional to the difference in intensity ΔI. The process is nonlinear, and the surprise will decrease as the background mask is made more intense. This information based on local intensity differences is similar in spirit to textural parameters identified by previous authors [*Barber and LeDrew*, 1991; *Shokr*, 1991] and is called textural information, in keeping with the formal identification of $-lnp_c$ as a surprise in information theory.

If the experiment is extended and all pixels of a given intensity are allowed to appear simultaneously, it is clear that because the intensity clusters by ice type, there is a tendency to outline a particular structure within the imagery. Because these displayed pixels all have the same ΔI, the property that we are viewing is both integral and a function of the intensity we wish to view. Examination of (1) and (2) reveals that the integral properties of the distribution are conveyed by Q. It is therefore reasonable to ascribe lnQ to the structural information.

Alternatively, the reader might visualize the decomposition of information into the textural information inherent in a single isolated, say, multiyear, floe and into the structural information associated with the spatial distribution of such floes.

Clearly, there is a correlation between local texture of an ice type and its structure. If both were the same between ice types, there would be no basis on which to distinguish them. It has been shown [*Kerman*, 1999] that if the structural information is plotted against the textural information in what is called an information curve, distinct subsections exist within the plot. Such subsections represent explicitly the correlation between texture and structure. These subsections were identified with distinct ice types and form the basis for a segmentation by ice type. In summary, a comparison of different information properties within an image isolates individual ice-type substates within the mixture of ice types.

In this paper we wish to extend the concept of Gibbs informational properties to a one-dimensional analysis of the thickness of ice. The basic question we wish to answer with such an analysis is as follows: "Is there evidence of information states in the under-ice topography?". Further, because we have access to data where there is coincident radar imagery over a track where the thickness is known, we can further ask "Are there any commonalities between the information in imagery and that in the thickness field?" As shown below, the analysis demonstrates an unexpectedly high degree of similarity in the information in the two fields.

2. Ice Thickness

In this section we wish to examine the informational properties of the topography of the underside of an ice field. Primarily, we wish to examine the possibility of a Gibbs structure for thickness, the existence of a multifractal characteristic, and most important whether there is evidence of information states in the ice topography.

2.1. Measurement and Some Basic Statistics

For almost 4 decades nuclear submarines have been able to travel extended distances under the Arctic ice cover. The draft of the ice has been measured from these platforms by using an upwardly pointed echo sounder to measure the difference in range between the ice bottom and the submarine. A number of data sets are now available which provide one-dimensional transects under the ice. In this study we will confine ourselves to an analysis of the USS Gurnard data taken during the Arctic Ice Dynamics Joint Experiment (AIDJEX) experiment [*Wadhams and Horne,* 1980] and of the HMS Superb data taken during the 1987 Aircraft/Submarine Sea Ice Project (ARCTIC87) experiment [*Wadhams et al.,* 1991; *Comiso et al.,* 1991; *Wadhams and Comiso,* 1992]. The details of these experiments will not be repeated here.

From these experiments and other similar studies, two important statistical properties of the thickness field have been established. The first is the negative exponential probability distribution of ice thickness at deep drafts where only deformed ice exists [*Wadhams,* 1981], and the second is the scaling or fractal nature of the field [*Key and McLaren,* 1991; *Bishop and Chellis,* 1989; *Kerman and Wadhams,* 1990; *Wadhams and Davis,* 1994]. Below, it is shown that the analyses reported to date represent averages of these properties over all ice types and that it is possible to find the same structures for various ice types in the entire ensemble. Specifically, it is useful to extend previous studies by testing whether the exponential property extends to the probability of thickness differences between neighboring drafts.

2.2. Gibbs Property

As discussed above, it is known that the conditional probability of thickness itself, given that our reference depth is the water level, is exponential [*Wadhams,* 1981]. As shown in Figure 1, the (conditional) probability distributions of thickness differences for both the Gurnard and the Superb data sets are also negatively exponential. However, the distributions are a function of the depth from which local thickness differences is computed. It is clear from this analysis that Wadhams' result for the probability distribution of ice depth can be seen as a special case that uses the waterline as a reference level compared to a generalized reference depth.

The starting depth, which in Figure 1 was 4.8 m, was chosen for display because it exceeded a depth where undeformed, or at least weakly fractured, ice would be considered to exist. It is important to point out that the result presented in Figure 1 is also a function of the horizontal spatial separation; a long enough separation along the submarine's track is required to minimize the serial correlation created in the original data where the sampling distance is smaller than the sonar beam averaging distance.

The existence of a depth dependency to the thickness difference distributions is important because it essentially leads us to expect that different information exits at different depths. Otherwise, there would be no basis for discrimination of ice type in the topography record. The existence of a negative exponential form for the conditional probability given by

$$-lnp_c(\Delta h; h) = lnQ + \beta \Delta h \tag{3}$$

allows us to expect that an information decomposition is possible. The symbolism is the same as that chosen for (1) and (2) but it is understood that parameters refer implicitly to ice thickness only. As before, the structure or partition function Q is determined from the intercept of the empirical data of Figure 1 and β is calculated as the slope of the conditional distribution at a given depth. The two parameters are necessarily functions of the depth at which the (conditional) distribution is computed.

The variability of these two parameters is shown in Figure 2 as functions of depth for the two experiments. In Figure 2, the texture information is almost identical between the two experiments, but there is significant variation between the structural information. Physically, the AIDJEX experiment was conducted in the Beaufort Sea in transitional ice from nearshore to open ocean pack ice, whereas the ARCTIC87 experiment represents open ocean conditions. A comparison of the joint properties of the intercept and slope with depth as a parameter is presented in section 4 in conjunction with the discussion of information in the thickness field.

As with the analysis of Kerman [1999], (3) allows for a decomposition of information. Consider an ensemble of thickness differences averaged at depth h by multiplying both sides of (3) by the conditional probability and dividing by the probability density of that depth. The result is

$$< -lnp_c >= lnQ + \beta < \Delta h > \tag{4}$$

As with (2), the two right-hand terms represent structural and textural contributions to the total information in the one-dimensional thickness profile. For convenience, here in terms of ice topography and elsewhere when referring to imagery, the average differences in thickness and intensity are incorporated in the definition of β. The result is that we can consider β and lnQ as the (average) textural and structural information. We now wish to examine the under-ice topography for potential fractal characteristics and, particu-

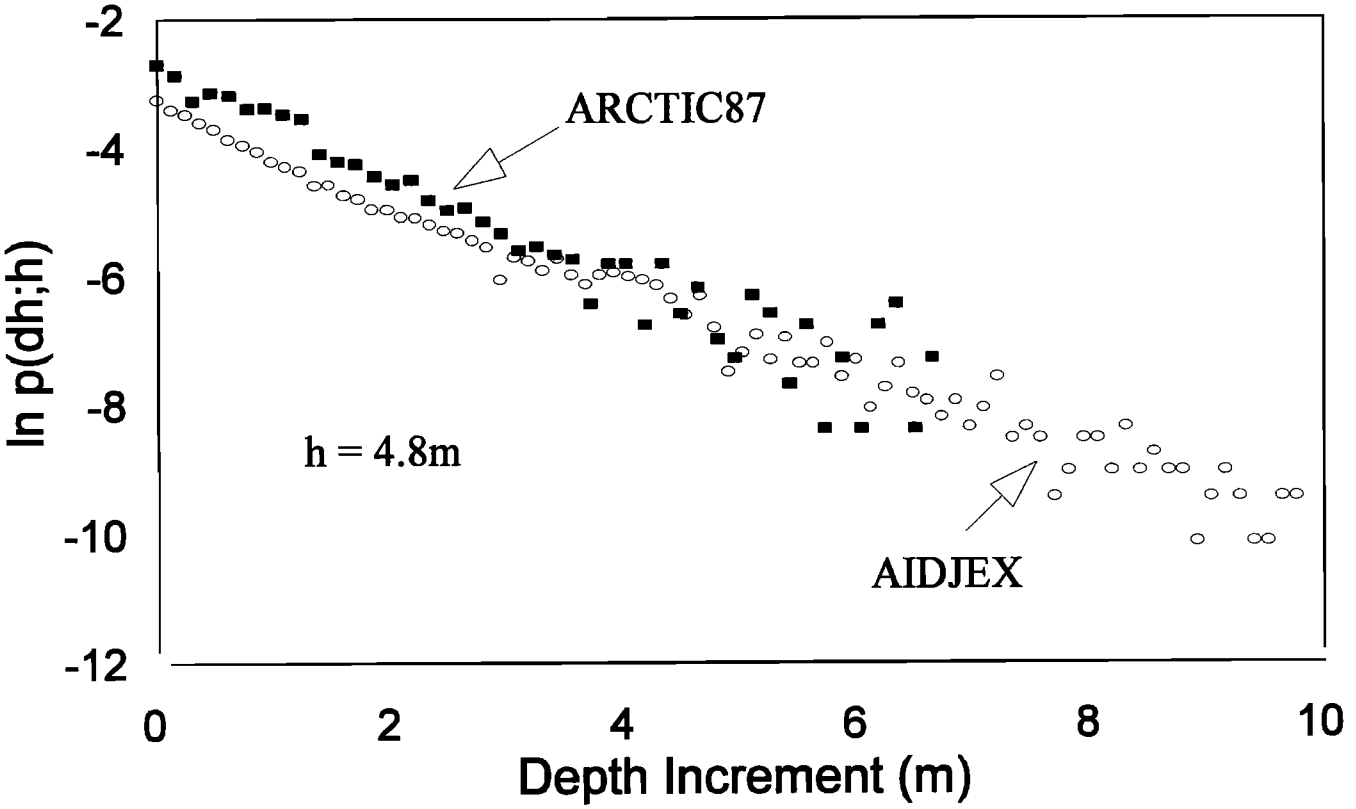

Figure 1. Example of the Gibbs property for thickness of ice. The probability of thickness increments from 0 to 10 m below a depth of 4.8 m for both experimental data sets is a negative exponential.

larly, whether there is evidence of a depth dependence for the fractal property.

2.3. Scaling (Fractal) Property

As mentioned earlier, a number of studies have shown that the ice thickness field has a scaling/fractal property [*Bishop and Chellis,* 1989; *Key and McLaren,* 1991; *Kerman and Wadhams,* 1990; *Wadhams and Davis,* 1994]. The study by Kerman and Wadhams identified that the topography was multifractal in terms of an energy-related variable (singularity strength) [*Feigenbaum et al.,* 1986] but did not ascribe any physical significance to that variable. We next wish to examine the scaling properties of Q and β derived from ice thickness profiles.

Consider an analysis of the conditional probability for different (horizontal) separations λ for a single initial depth for all $\Delta h \geq 0$. The results of such a calculation are presented in Figure 3. Clearly, the integrated conditional probability p_c has the scaling property in that it varies as λ^{-m} for all thickness variations and for separations of 10 to 100 m. Because this integrated property is inversely related to Q, it is concluded that a multifractal property, $Q \sim \lambda^{-m(h)}$, exists for the partition function of the ice topography. It is further argued that β is invariant in λ because the results (not shown) for conditional probability for different Δh remain parallel in λ (see Figure 4 for the similar property for SAR imagery, discussed below). Accordingly, it is concluded, just as was found for SAR imagery, that Q has a scaling property but β is scale invariant. In other words, the structural information has a scaling (fractal) characteristic but the textural information is the same, irrespective of scale. In order to understand this result intuitively in terms of imagery, note in Figure 5 that the texture of, say, multiyear floes is the same independent of floe size but that there is a size distribution and spatial arrangement of such floes.

The Gibbs and multifractal properties of ice thickness can be summarized by

$$p_c(\Delta h; h) = [Q_1(h)\lambda^{m(h)}]^{-1} exp[-\beta(h)\Delta h] \quad (5)$$

where Q_1 is the structure function for $\lambda = 1$ as implied in (4).

3. SAR imagery

It was shown by Kerman and Johnson [1998] that a scaling, Gibbs property exists in wintertime C and L band SAR imagery of sea ice taken over the Beaufort Sea. Figure 4 jointly presents the essence of those results for a given scene of ~8 by 10 km with pixel sizes of ~10 m on a side. The hyperbolic, power law behavior both at individual intensity differences and all

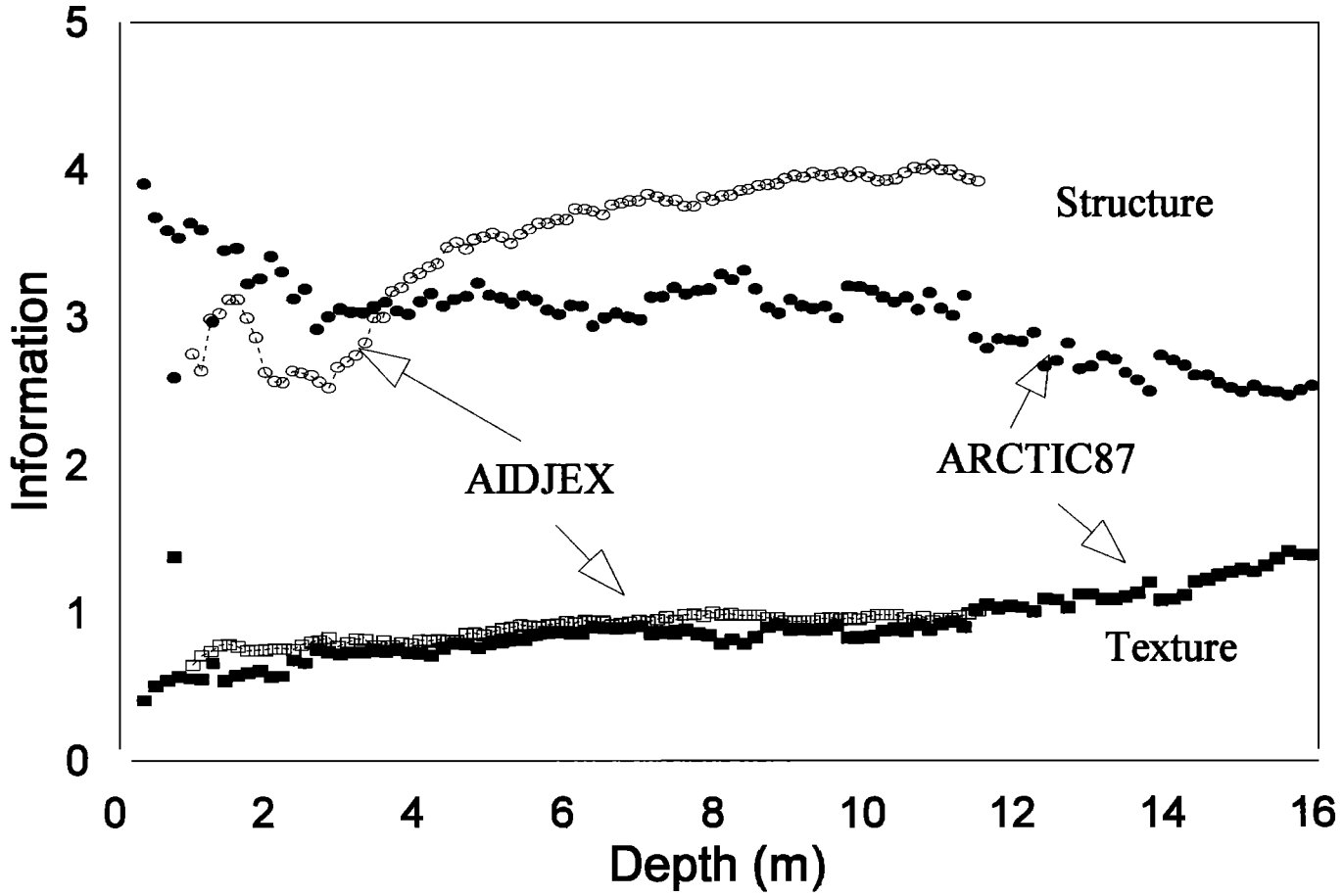

Figure 2. Distribution of textural β and structural information lnQ as a function of depth for the two experiments (Arctic Ice Dynamics Joint Exponent AIDJEX and 1987 Aircraft/Submarine Sea Ice Project ARCTIC87).

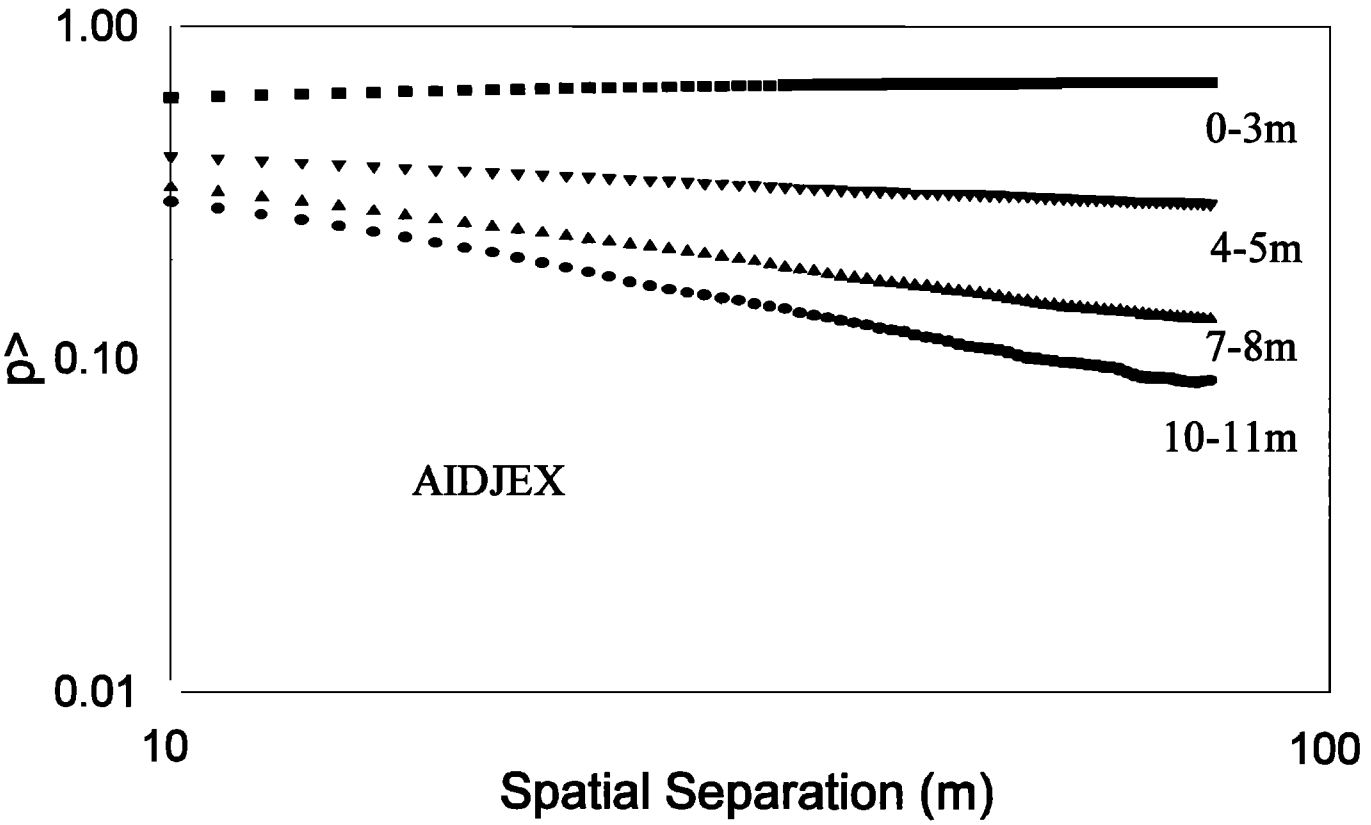

Figure 3. The probability $p_>$ that a neighbor will be even thicker as a function of the separation between neighbors, λ. Note that ice of thickness less than 4 m does not show evidence of a scaling property.

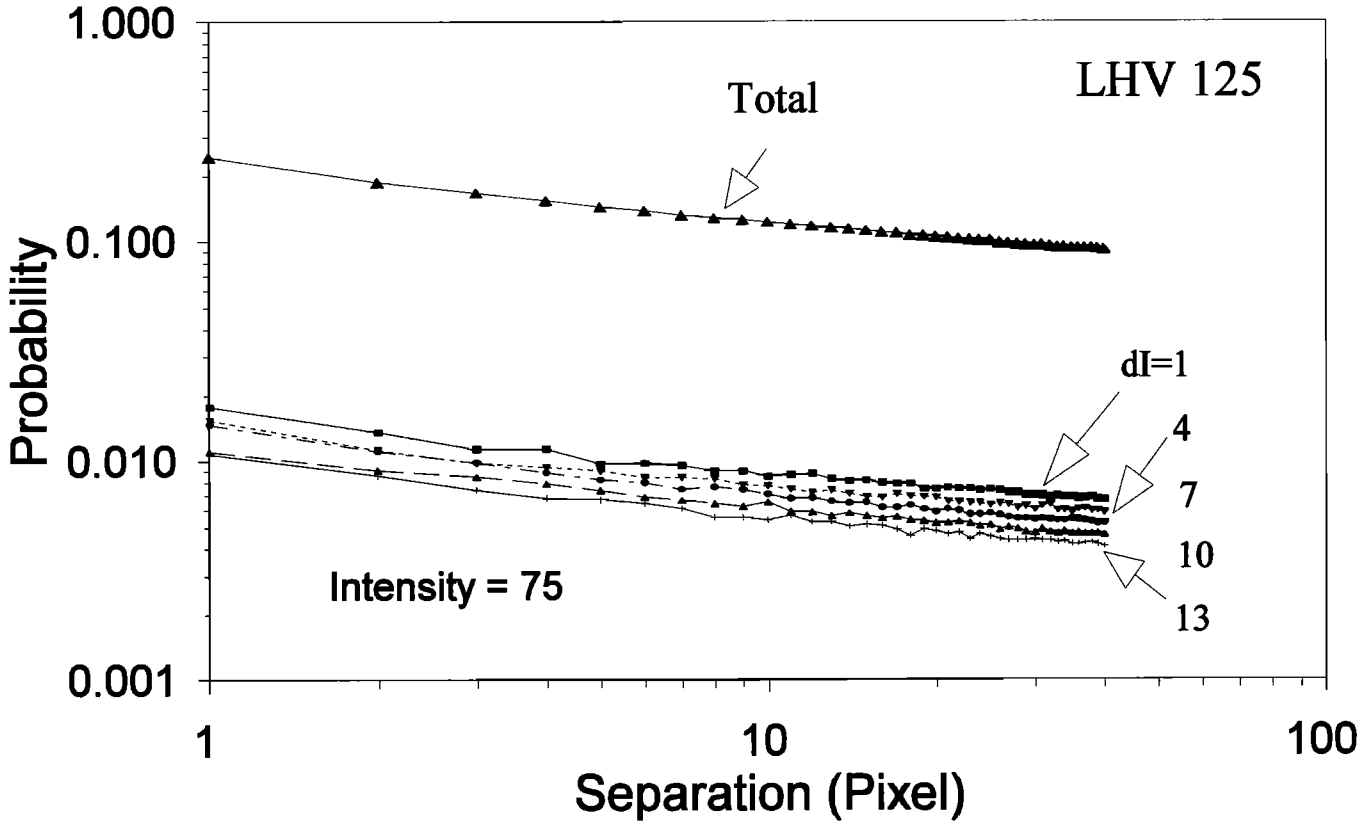

Figure 4. Evidence of the scaling property of the conditional probability of intensity difference for a given intensity. The imagery is from a wintertime experiment in the Beaufort Sea (scene 125, L band, HV polarization, intensity=75) (see text). The top curve corresponds to the form of data in Figure 3. Note that the Gibbs property (conditional probability of a given intensity difference) seen at any separation λ is invariant with separation implying that β is scale invariant.

differences (Figure 4, top curve) confirms the scaling properties at a given intensity. Further, it is noted that the (logarithmic) spacing between the intensity difference distributions remains constant for different spatial separations. This constant spacing is related to the existence of an exponential distribution for the intensity differences between neighboring pixels. This leads to the conclusion, mentioned in section 2.3, that the textural parameter β is scale invariant whereas the structural parameter Q is scaling.

In the ARCTIC87 experiment, imagery was collected by an aircraft-borne SAR operating the X band STAR 2 system of Intera Technologies. Two images, one taken over Arctic pack ice west of Greenland and another taken near the northern tip of Greenland, are presented in Figure 5. As shown in Figure 6 for one of these images, there is strong support for the existence of a Gibbs property in this data as in previous imagery analyzed. Although not shown, the scaling property (see Figure 4) is also present in the X band imagery of this experiment as it was for the C and L band Beaufort Sea imagery reported earlier.

4. Informational Equivalence

As discussed above, (2) and (4) imply a decomposition of the total information at a given value of intensity or thickness into structural (lnQ) and textural (β) information. Further, it was mentioned in the introduction that subranges exist in sea ice imagery [*Kerman*, 1999] where the structural and textural information derived from the imagery is correlated, with relatively distinct points of demarcation between these ranges at points called "phase-transitions". We now wish to jointly examine the covariational properties of the structural and textural information for both the one-dimensional thickness data and the simultaneous two-dimensional imagery.

The various information types for both the imagery and ice thickness taken during the Arctic pack ice and north Greenland Sea legs of ARCTIC87 are presented in Figure 7a,b. (The textural information for the thickness data has been arbitrarily amplified by a factor of 2.5 to place it in the approximate range of that from the imagery.) Several subranges with phase transitions are

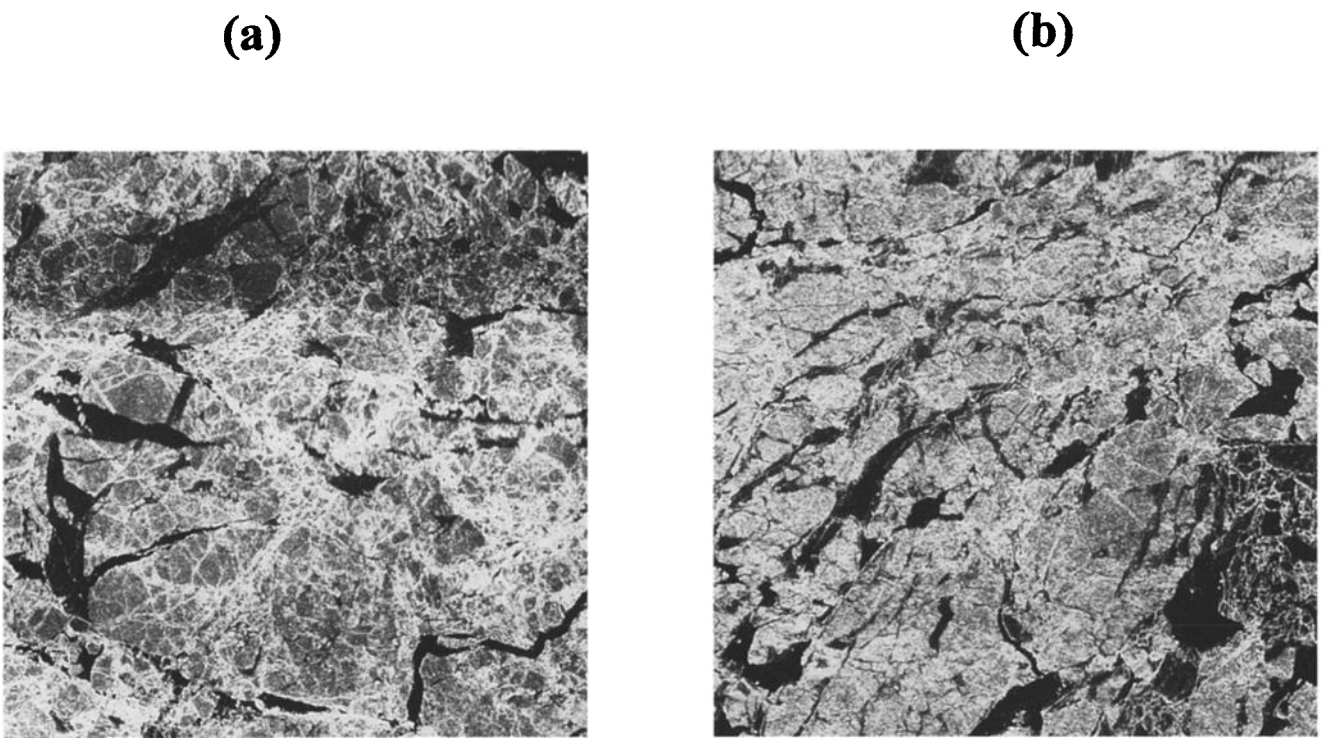

Figure 5. X band imagery taken in ARCTIC87 (a) over the Arctic pack ice and (b) in the northern Greenland Sea.

evident in the SAR information comparison: a steeply descending branch for small textural information, an approximately constant branch for medium β, and a weakly decreasing branch at higher textural information.

To understand the physical significance of each branch, consider one of the SAR images, say, Figure 5a. The tonal dynamic range divides into essentially three ice types, which can be roughly categorized as black (open water/new or first-year ice), gray (mostly thick multiyear ice) and white (ridged first and multiyear ice), with a darkened swath across the upper part of the image. From the corresponding information curve (Figure 7a) for this imagery, it is also apparent that there are three subranges. It was verified that the apparent ice types seen in Figure 5a correspond to the different states implied in Figure 7a by varying the threshold in an image viewer near the critical intensities (phase transitions) between each subrange in Figure 7a. We thus conclude that the information states correspond to open water/new ice, multiyear, and ridged ice.

From the thickness information curves of Figure 7a the phase transition points at the apparent end of the two descending branches for low and high textural information occur at depths of ~1 and 4 m. These depths are significant in terms of an analysis of the Gurnard data conducted by Wadhams and Horne [1980], and subsequently by McLaren [1989] for other thickness data from submarine platforms. They identified approximate boundaries between ice types by ice thickness which can be summarized as follows: thin, young ice ($h < 0.7\ m$), medium, young ice ($0.7\ m < h < 1\ m$); thick, young (first year) ice ($1\ m < h < 2\ m$); level, second-year, and multiyear ice ($2\ m < h < 4\ m$); level, multiyear, and ridged, deformed ice ($3\ m < h < 8\ m$).

From their analysis it is reasonable to relate the (leftmost) lowest textural information subrange for thickness in Figure 7a, corresponding to $0 < h < 1\ m$, with young and medium ice. This identification is consistent with that of new ice for that branch corresponding to the lowest textural information in the SAR imagery. Further, it is appropriate to identify the (rightmost) highest textural information subrange corresponding to thicknesses greater than 4 m with ridging, from the look-up tables of Wadhams and Horne [1980] and McLaren [1989]. It is noted that ridging ice type identification was also given to the corresponding branch of the information curve based solely on the imagery. The midtextural information region ($1\ m < h < 4\ m$) by the thickness association procedure corresponds to a number of identifiable ice types (thick first year, second year, and multiyear), all of which, while having a significantly richer texture than new ice, display their texture approximately uniformly compared to ridging. Accordingly, it is concluded that the middle subrange of both the ice information curves for imagery and thickness corresponds to a thick flat, homogeneously textured ice type in general.

The two critical thicknesses, 1 m and 4 m, correspond physically to a real division between three modes of for-

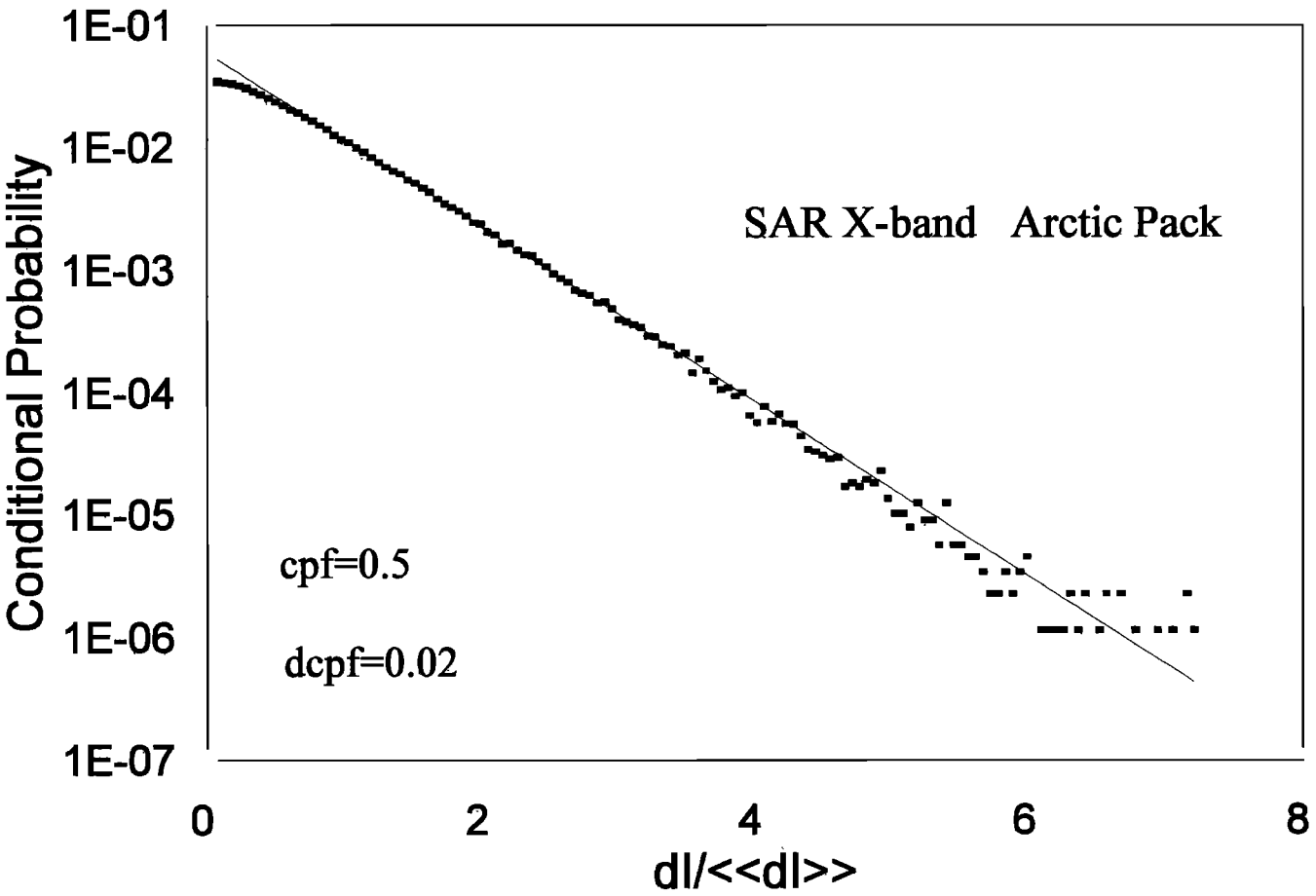

Figure 6. Example of the Gibbs property for the imagery of Figure 5a at an intensity corresponding to the cumulative probability for intensity (cpf) = 0.5. The data have been averaged over a window of intensity corresponding to $0.48 < cpf < 0.52$.

mation of the ice. Multiyear ice grows to a maximum thickness of ~4 m after many years, so ice thicker than 4 m is overwhelmingly ice that has gained its thickness through deformation into ridging. New ice that begins to grow at the beginning of winter will have reached a thickness of a little more than 1 m by April (Gurnard) or May (Superb) of the following year. Therefore ice between 1 m and 4 m thick is mainly composed of undeformed first-year and multiyear ice that has grown thermodynamically, although some ridged ice, of necessity, falls into this thickness range. Ice less than 1 m thick began to grow more recently than the start of the current winter, by the refreezing of leads, which were themselves opened by the mechanical action of the fracture and divergence of the ice cover. Therefore ice less than 1 m thick, although it may be undeformed, is the end product of a mechanical process in the ice rather than a purely thermodynamical process. The fact that the curves of Figure 7 show phase transitions at thicknesses which correspond to real physical transitions in the nature of the ice cover is a highly significant result.

A similar analysis (Figures 5b and 7b; northern Greenland Sea) indicates again that there are three ice types. Overall, there is a tendency in the imagery of Figure 5b for more open water/new ice in less linear features than in Figure 5a. The information curve (Figure 7b) for this image resembles that for the Arctic pack ice. We note that there exists a well-defined extension of the new ice substate (low textural information) below that of the multiyear ice substate. The latter appears as a nearly constant state of structural information. The extension of the young ice substate can be perceived also in the information curve for the thickness data. No explanation has been found yet for this feature.

In conclusion, there exist identifiable ice types in the imagery, which have associated information states. Further, information states in the thickness data can be identified with ice type on the basis of the ice depth corresponding to the phase transitions; and, importantly, the two sets of information states separate the ice field into the same kinds of identifiable ice types. In the sense of identifying identical ice types, the information from the imagery is equivalent to that from the under-ice topography.

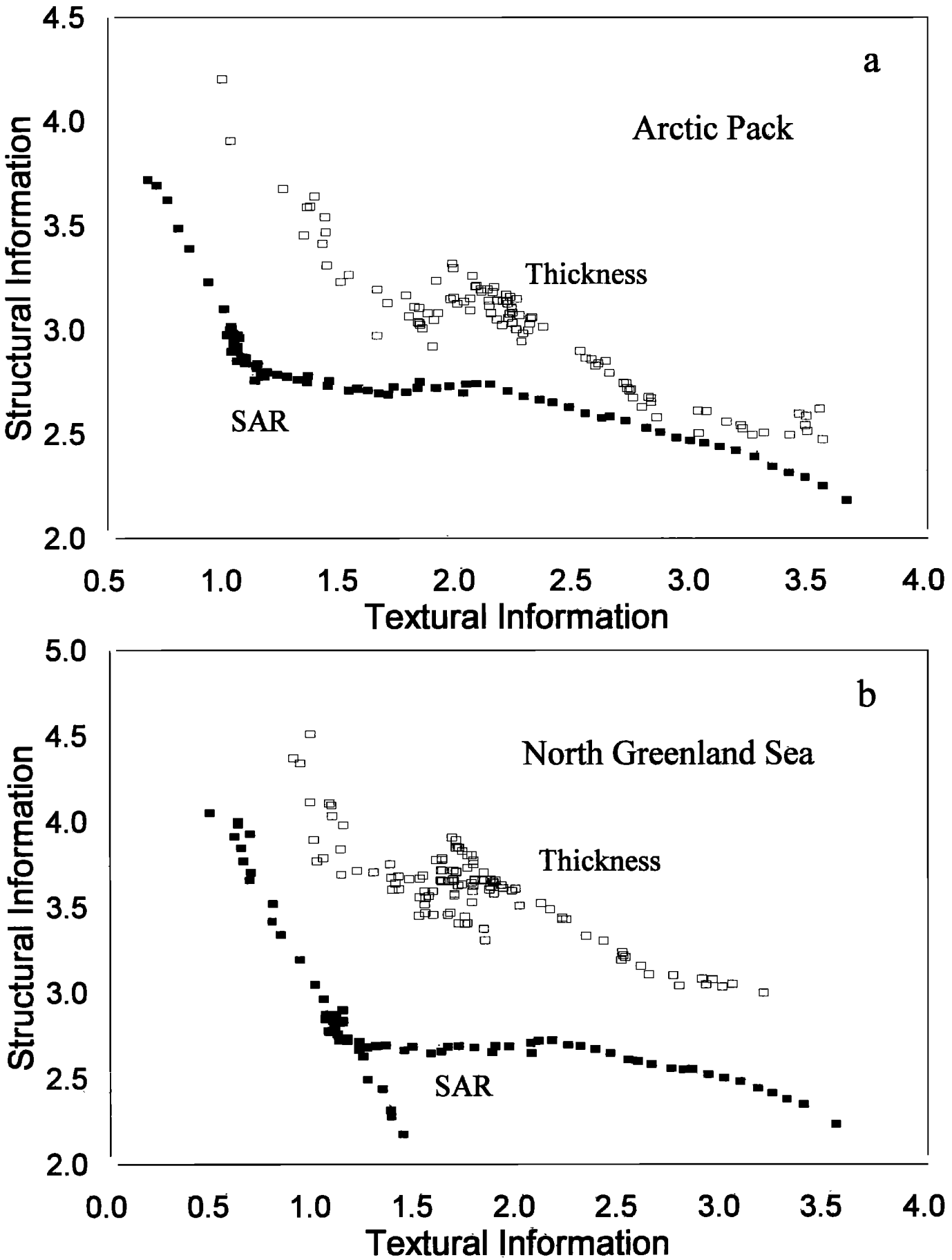

Figure 7. Information curves (structural (lnQ) versus textural information (β) for synthetic aperture radar (SAR) imagery and thickness in (a) the Arctic pack ice and (b) in the northern Greenland Sea. The textural information for thickness has been multiplied by a factor of 2.5 to correspond to the range of the textural information from the SAR imagery.

5. Discussion

The analysis described above has provided a number of useful results. It is clear that both the SAR imagery and ice topography possess the Gibbs property; that both can have this Gibbsian property parameterized in terms of basic variables (intensity and thickness); that a multifractal scaling relationship of these parameters exists for both data sets; and, most importantly, physically meaningful information states for each mode of data can be identified with common ice types. Of these, the important result operationally is that there is an equivalent relationship between the structure information of subclasses of a limited range of texture in both (X band) imagery and the thickness profile of the sea ice.

Perhaps the most surprising result of the entire analysis is that the information curve diagram for the thickness data has a form very similar to that for the imagery. The comparison holds for both images used here. The similarity in form between the information plots implies that the information is equivalent in the mathematical sense that a transformation can be found to represent one function in terms of another. It is important to note that a priori there is no reason to expect such a result. For example, if another radar frequency and/or polarization had been used to interrogate the ice field, a different information curve [*Kerman and Johnson,* 1998; *Kerman,* 1999] would have been observed which might not be obviously similar in form to that of the thickness analysis. However, as long as one can find a group of affine transformations to map one segment in the imagery curve to another in the thickness analysis, it is consistent to speak of informational equivalence.

While the existence of apparent equivalence is interesting in itself, several cautionary notes need to be made. The first is that there is no reason to believe that the entire information curve for, say, thickness, can be recovered from that of imagery of any arbitrary radar frequency. Since the thickness profile results primarily from the fracture associated with alternating compression and tension in the ice field, to capture most of the thickness information requires a sufficiently long radar wavelength which penetrates the ice in order to sense fracture within the ice, as opposed to another which senses mostly surface roughness changes. Because the current radar imaging satellites (Radarsat, ERS) use a longer wavelength than the X band system described here, there exists the possibility of improved sensitivity with these systems for determining information states in SAR imagery.

The equivalence of information suggests that the statistics of the thickness of an ice field may be estimated from radar imagery in a number of possible ways. This is of significant importance since there is an operational need to be able to synoptically map sea ice thickness in the polar regions; yet direct sounding of sea ice by electromagnetic means from satellites is not possible because of the ice's electrical conductivity. The first method for exploiting the results of this paper recognizes that the cumulative probability distribution of ice type in the image must be that of the under-ice probability. A simple way to proceed is to determine the phase transition points from imagery, note the cumulative probability to which their intensities correspond, and ascribe the abundance of underwater ice type and thickness properties accordingly. If a simulated realization is required, the empirical conditional probability distribution (equation 5) for different ice types offers the possibility of a Monte Carlo simulation. Another possible simulation method could be built around the generation of networks within the scene associated with ice types [*Kerman,* 1998a,b]. To extend this work to other imagery, it is desirable to develop a set of empirical affine transformations to map the information states of the imagery to those of ice thickness.

The main unanswered question associated with the equivalence of the information is "What aspect of the imagery is providing the information that is equivalent to that for thickness"? This questions begs another, "Is there some variable within the imagery that carries information equivalent to the thickness field"? The answer appears to be quite simple.

Consider the analogy of a (defoliated) forest viewed from above. Consider the collection of trees making up the forest as an ensemble of fractal networks. It is reasonable to expect that the extent of the (invisible) root structure of each tree will have some relationship to the tree's (visible) size and fractal network. By analogy, it is plausible that the ice thickness profile ("roots" of the ice field) will be related to the fractal networks ("trees") identified in SAR imagery analyzed by Kerman and Johnson [1998]. Those networks of similitude in the imagery are a surface manifestation of the same compressive and tensile forcing of the ice field that produces the ice.

This analogy between ice thickness and network length has been examined further [*Kerman,* 1998b,c]. It was shown that the lengths of individual networks, defined using a measure derived from the Gibbs property of the imagery, have the same negative exponential distribution as the thickness data. It is argued there that the energy associated with pushing fractured ice down further against buoyancy and the energy required to further lengthen existing fracture have an identical negative exponential form in terms of thickness and fracture length, respectively. The answer to the above questions appears to be that what is Gibbsian, and multifractal and possesses equivalent information between SAR imagery and the ice thickness is the fossil evidence of fracture in networks within the imagery.

References

Barber, D.G., and E.F. LeDrew, SAR sea ice discrimination using texture statistics: A multivariate approach, *Photogramm. Eng. Remote Sens., 57*(4), 385-395, 1991.

Bishop, G.C., and S.E. Chellis, Fractal dimension: A de-

scriptor of ice keel surface roughness, *Geophys. Res. Lett., 16*(9), 1007-1010, 1989.

Comiso, J.C., P. Wadhams, W. Krabill, J. Crawford, and W. Tucker, Top/bottom multisensor remote sensing of Arctic sea ice, *J. Geophys. Res., 96*(C2), 2693-2711, 1991.

Drinkwater, M.R., R. Kwok, D.P. Winebrenner, and E. Rignot, Multifrequency polarimetric synthetic aperture radar observations of sea ice, *J. Geophys. Res., 96*(C11), 20,679-20,698, 1991.

Duxbury, P.M., and Y. Li, Scaling theory of the strength of percolation networks, in *Disorder and Fracture, NATO ASI Ser. B, Physics*, v235, edited by J.C. Charmet, S. Roux, and E. Guyon, Plenum, New York, 1990.

Falco, T., F. Francis, S. Lovejoy, D. Schertzer, B. Kerman, and M. Drinkwater, Universal multifractal structure of SAR radar images of sea ice, *IEEE Trans. Geosci. Remote Sens., 34*(4), 906-914, 1996.

Feder, J., *Fractals*, Plenum, New York, 1988.

Feigenbaum, M.J., M.H. Jensen, and I. Procaccia, Time ordering and the thermodynamics of strange sets: Theory and experimental tests, *Phys. Rev. Lett., 57*(13), 1503-1506, 1986.

Holmes, Q.A., D.R. Nuesch, and R.A. Shuchman, Textural analysis and real-time classification of sea-ice types using digital SAR data, *IEEE Trans. Geosci. Remote Sens., 22*(2), 113-120, 1984.

Kerman, B.R., A damage mechanics model for sea ice imagery, *Global Atmos. Ocean Syst., 6*, 1-34, 1998a.

Kerman, B.R., On the relationship of ice pack thickness to the length of connectivity trees in SAR imagery, in *Proceedings of 14th International Symposium on Ice, Ice in Surface Waters*, vol.2, edited by H.T. Shen, Clarkson Univ., Potsdam, N.Y., 1998b.

Kerman, B.R., Segmentation of sea ice imagery based on a scaling, Gibbs probability measure of similitude, in *Fractals and Beyond: Complexities in the Sciences*, edited by M. N. Novak, World Sci., River Edge, N.J., 1998c.

Kerman, B.R., Information states in sea ice imagery, *IEEE Trans. Geosci. Remote Sens., 37*(3), 1435-1446, 1999.

Kerman, B.R., and K. Johnson, Properties of a probability measure for sea-ice imagery, *Global Atmos. Ocean Syst., 6*, 35-92, 1998.

Kerman, B.R., and P. Wadhams, Multifractal structure of the underside of ice, paper presented at *Conference Wavelets, Fractals and Fourier Transforms*, Dept. Applied Math. and Theor. Phys., Univ. Cambridge, Cambridge, England, 1990.

Key, J., and A.S. McLaren, Fractal nature of the sea ice draft profile, *Geophys. Res. Lett., 18*(8), 1437-1440, 1991.

Kwok, R., G. Cunningham, and B. Holt, An approach to identification of sea ice types from spaceborne SAR data, in *Microwave Remote Sensing of Sea Ice, Geophys. Monogr. Ser.*, vol. 68, edited by F. Carsey, pp 355-360, AGU, Washington, D.C., 1992.

McLaren, A.S., The under-ice thickness distribution of the Arctic Basin as recorded in 1958 and 1970, *J. Geophys. Res., 94*(C4), 4971-4983, 1989.

Palmer, A.C., and T.J.O. Sanderson, Fractal crushing of ice and brittle solids, *Proc. R. Soc. London, ser. A, A433*, 469-477, 1991.

Pentland, A.P., Fractal-based description of natural scenes, *IEEE Trans. Pattern Anal. Mach. Intel., 6*(6), 661-674, 1984.

Ramsay, B., M. Manore, L. Weir, K. Wilson, and D. Bradley, Use of Radarsat data in the Canadian Ice Service, *Can. J. Remote Sens., 24*(1), 36-42, 1998.

Shannon, C., A mathematical theory of communication, *Bell Syst. Tech. J., 27*, 379-423, 1948.

Shokr, M.E., Evaluation of second-order texture parameters for sea ice classification from radar images, *J. Geophys. Res., 96*(C6), 10,625-10,640, 1991.

Wadhams, P., Sea ice topography of the Arctic Ocean in the region 70°W to 25°E, *Philos. Trans. R. Soc. London, Ser. A, A302*, 1464-1504, 1981.

Wadhams, P., Sea ice thickness distribution in the Greenland Sea and Eurasian Basin, May 1987, *J. Geophys. Res., 97*(C4), 5331-5348, 1992.

Wadhams, P., and J. C. Comiso, The ice thickness distribution inferred using remote sensing techniques, in *Microwave Remote Sensing of Sea Ice, Geophys. Monogr. Ser.*, vol 68, edited by F. Carsey, pp. 375-383, AGU, Washington, D.C., 1992.

Wadhams, P., J.C. Comiso, J. Crawford, G. Jackson, W. Krabill, R. Kutz, C.B. Sear, R. Swift, B. Tucker, and N.R. Davis, Concurrent remote sensing of Arctic sea ice from submarine and aircraft, *Int. J. Remote Sens., 12*(9), 1829-1840, 1991.

Wadhams, P., and N.R. Davis, The fractal properties of the underside of Arctic sea ice, in *Marine, Offshore and Ice Technology*, edited by T.K.S. Murthy, P.A. Wilson, and P. Wadhams, pp. 353-363, Comput. Mech., Billerica, Mass., 1994.

Wadhams, P., and R.J. Horne, An analysis of ice profiles obtained by submarine in the Beaufort Sea, *J. Glaciol., 25*, 401-424, 1980.

J. Comiso, Oceans and Ice Branch, NASA Goddard Space Flight Center, Code 971, Greenbelt, MD 20771. (comiso@joey.gsfc.nasa.gov)

N. Davis and P. Wadhams, Scott Polar Research Institute, University of Cambridge, Cambridge, England CB2 1ER. (nrd10@cam.ac.uk;pw11@cam.ac.uk)

B. Kerman, Atmospheric Environment Service, Canada Centre for Inland Waters, Burlington, Ontario, Canada L7R 4A6. (bryan.kerman@cciw.ca)

(Received June 15, 1998; revised June 2, 1999;
accepted June 9, 1999.)